Average symbol error rate analysis of reconfigurable intelligent surfaces-assisted free-space optical link over log-normal turbulence channels

Duong Huu Ai, Cong Dat Vuong, Dai Tho Dang
Vietnam-Korea University of Information and Communication Technology, The University of Danang, Danang, Vietnam

Article Info

Article history:

Received Nov 5, 2021
Revised Aug 5, 2022
Accepted Sep 1, 2022

Keywords:

Average symbol error rate
Free-space optical communications
Log-normal turbulence channels
Quadrature amplitude modulation
Reconfigurable intelligent surfaces

ABSTRACT

Optical wireless communication (OWC) has attracted significant interest recently in academia and industry. Free-space optical (FSO) communication systems are where free space acts as a communication channel between transceivers that are line of sight (LOS) for the successful transmission of optical signals. The FSO transmissions through the atmosphere, nevertheless, bring significant challenges, besides the uncertainty of atmospheric channels, especially the signal fading due to the atmospheric turbulence, attenuation and pointing errors caused by the random beam misalignments between transceivers, signal obstruction due to buildings or trees can pre-vent the transmitted message to reach the destination. This study theoretically investigates the average symbol error rate (ASER) of reconfigurable intelligent surfaces (RIS) assisted FSO link over log-normal turbulence channels. The RIS effect is examined by considering the influence of link distance, transmitted optical power, and quadrature amplitude modulation (QAM) scheme on the ASER.

Corresponding Author:

Duong Huu Ai
Vietnam-Korea University of Information and Communication Technology, The University of Danang
Danang, Vietnam
Email: dhai@vku.udn.vn

1. INTRODUCTION

Free space optical communication systems are where free space acts as a communication channel between transceivers that are line of sight (LOS) for the successful transmission of optical signals. The critical advantage of free-space optical (FSO) is flexibility in designing optical network architectures at very high speeds, at tens and hundreds of Gbit/s rates [1]. Atmospheric propagation factors, for example, fog, haze, snow, and rain, are the most critical disadvantages. The deployment of FSO systems faces some challenging problems: negative effects scattering, turbulence, absorption, and even misalignment between transmitter and receiver. A new procedure was presented in [2]–[7] for deriving the statistical distribution of pointing errors and turbulence in current works.

Currently, deploying optical relay nodes is the only possible resolution to the obstruction problem. This approach is expensive and inconvenient because of additional hardware deployment [8]–[12], [13]–[17]. Reconfigurable intelligent surfaces (RIS) are electromagnetic devices with electronically controllable characteristics. RIS able to refract, extinct, scatter or reflect the incoming signal by influencing the incoming signal's phase, polarization, and amplitude. RIS module design is based on its application. The RIS module includes multiple mirrors on a planar array. It directs the incoming signal toward a targeted area and reconfigures the transmission channel [18]–[24]. It helps wireless networks have many benefits over vying technologies. Besides, RIS consumes low power and is constructed with electronically controllable components. Therefore, it has become an area of current research interest. Materials for reconfigurable meta-surfaces often have optical properties modulated by an optical stimulus, mechanical, thermal, or external electrical. Conductive oxide materials, for example, indium tin oxide (ITO) in Figure 1. It includes four layers, i.e., a metal-semiconductor conductive oxide-metal (Au-Al2O3-ITOAu) setup. Upon applying a positive (negative) voltage bias, the free charges of the ITO layer accumulate (deplete) at the semiconductor-ITO interface. This variation of the charge accumulation layer causes a significant change in the refractive index of the ITO layer, which in turn alters the phase of the reflected electromagnetic waves. Similarly, graphene has been shown to exhibit significant charge carrier-dependent modulation for THz to near Infrared radiation (IR) wavelengths if an electrical field is applied [25].

This study introduces a theoretical investigation of the average symbol error rate (ASER) analysis of RIS-assisted FSO link. We theoretically analyze the ASER of signal-to-noise ratio (SNR) of RIS assisted FSO link over log-normal turbulence channels. The remainder of the study is presented as the following. Section 2 shows system descriptions and channel models. Section 3 presents the closed-form statistical analysis. The numerical results and discussions are shown in section 4. Finally, the study is included in section 5.

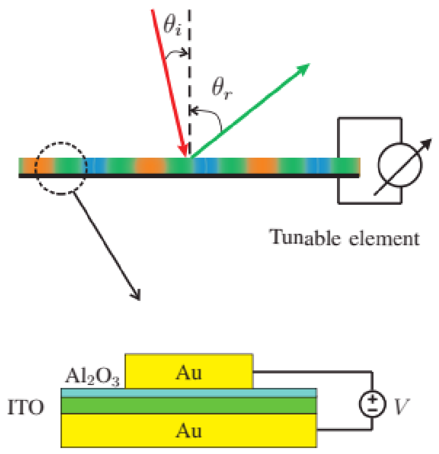

Figure 1. Schematic illustration of the optical RIS technology

2. SYSTEM AND CHANNEL MODELS

2.1. System model

The RIS-assisted FSO link environment under study is presented in Figure 2. Nodes S and D are the source and destination nodes, respectively. The signal is from node S. After the signal reflects on a RIS element, it is transmitted to D. S and D do not directly link because of obstructions.

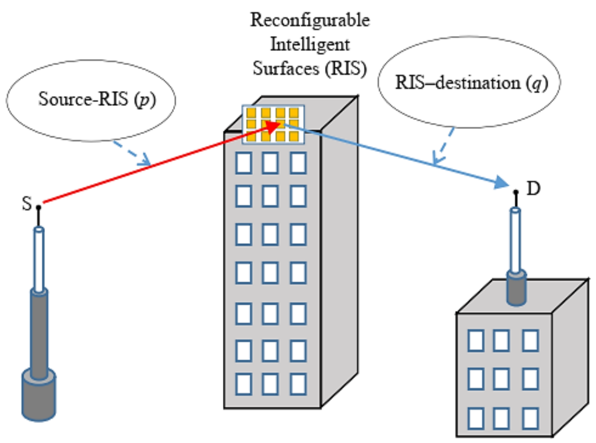

Figure 2. A model of RIS-assisted FSO system

The RIS module is placed at an appropriate position in the building. It reflects the incoming signal. Besides, it assures that transferred light reaches the receiver without being blocked. We assume that both transmitted and reflected channels exhibit weak turbulence levels, and the light intensity over them undergoes the same attenuation level. It is also assumed that, at each receiving end, the detectors face similar pointing errors. In the case under study, we assume there are no pointing errors.

2.2. The log-normal channel

Because of atmospheric conditions, one optical wave beam is deformed when it moves via the atmosphere. Three main signal factors impair the FSO link: atmospheric turbulence, attenuation, and pointing errors. The atmospheric turbulence caused by the irradiance fluctuation represents signal scintillation. Many models have been proposed for representing the atmosphere-induced turbulence. For weak turbulence conditions, *h(t)* is considered a spontaneous process according to log-normal distributions. The probability density function (pdf) of the irradiance intensity in the weak turbulent is given by [14].

$$f_h(h) = \frac{1}{X\sigma_S\sqrt{2\pi}} exp\left(-\frac{[ln(h)+0.5\sigma_S^2]^2}{2\sigma_S^2}\right) \tag{1}$$

where σ_S is the scintillation index, and is defined at [13] as $\sigma_S = exp(w_1 + w_2) + 1$; where

$$w_1 = \frac{0.49\sigma_2^2}{(1+0.18d^2+0.56\sigma_2^{12/5})^{7/6}} \tag{2}$$

$$w_2 = \frac{0.51\sigma_2^2(1+0.69\sigma_2^{12/5})^{-5/6}}{1+0.9d^2+0.62d^2\sigma_2^{12/5}} \tag{3}$$

In these equations, $d = \sqrt{kD^2/4L}$ where, $k = 2\pi/\lambda$ is optical wave number, λ is wavelength, L is link distance, D is radius of a circular receiving aperture, σ_2 is Rytov variance. Assuming that spherical wave propagation is defined:

$$\sigma_2^2 = 0.492C_n^2k^{7/6}L^{11/6} \tag{4}$$

In [10], C_n^2 is the refractive-index structure parameter.

3. CLOSED-FORM STATISTICAL ANALYSIS

3.1. End-to-end SNR

We assume the following: i) RIS module has a reflective function only, ii) the light cannot move through the RIS, and iii) the channel phases' perfect knowledge at the destination and RIS. The detected signal is determined as (5) [21]:

$$y = \sqrt{E_s}(p\eta e^{j\theta}q)x + w \tag{5}$$

where E_s is symbol energy, p is S-RIS, q is RIS-D, $\eta e^{j\phi}$ is characterizes the RIS element with η being its amplitude reflection coefficient and ϕ its induced phase [5], [14], x is transmitted symbols, y is received symbols, w is additive white Gaussian noise at the destination

The main goal is to reflect the original signal in such a way as to optimize signal reception at the D position. It can do by end-to-end SNR maximization. The value of SNR is computed by (6) [24]:

$$\gamma = \bar{\gamma}\left|p\eta e^{j\phi}q\right|^2 \tag{6}$$

where $\bar{\gamma} = \frac{E_s}{N_0}$ is the average SNR in both S-RIS and RIS-D sub-channels, and N_0 is the noise power spectral density.

3.2. PDF of the end-to-end SNR

The overall system's gain is $p\eta e^{j\phi}q$, where the quantity $\eta e^{j\phi}$ is deterministic in contrast to p and q, which are random variables. Denote $f_\gamma(\gamma)$, the SNR's PDF. It is evaluated as [26].

$$f_\gamma(\gamma) = \int_0^\infty f_{\gamma_p}(t) f_{\gamma_q}\left(\frac{\gamma}{t}\right)\frac{1}{t}dt \tag{7}$$

where $f_{\gamma_p}(\cdot)$ is PDF of the S-RIS, $f_{\gamma_q}(\cdot)$ PDF of the RIS-D.

We are assuming that weather conditions are constant. The channel' parts are represented by a distribution combination of turbulence levels and pointing errors. The resulting unified PDF, $f_{\gamma_i}(\gamma_i)$ is expressed as (8) [27]:

$$f_{\gamma_i}(\gamma_i) = \frac{1}{2\gamma_i\sigma_s\sqrt{2\pi}} exp\left(-\frac{(ln(\frac{\gamma_i}{\bar{\gamma}_i})+\sigma_s^2)^2}{8\sigma_s^2}\right) \tag{8}$$

where $i \in \{h, g\}$. We sequentially substitute γ_i by t and $\frac{\gamma}{t}$ in (8), and obtain $f_{\gamma_p}(t)$ and $f_{\gamma_q}(\frac{\gamma}{t})$ respectively as (9), (10):

$$f_{\gamma_p}(t) = \frac{1}{2t\sigma_s\sqrt{2\pi}} exp\left(-\frac{(ln(\frac{t}{\bar{\gamma}_p})+\sigma_s^2)^2}{8\sigma_s^2}\right) \tag{9}$$

$$f_{\gamma_q}(\frac{\gamma}{t}) = \frac{t}{2\gamma\sigma_s\sqrt{2\pi}} exp\left(-\frac{(ln(\frac{\gamma}{\bar{\gamma}_q t})+\sigma_s^2)^2}{8\sigma_s^2}\right) \tag{10}$$

where $\bar{\gamma}_p$ is average value of the SNRs γ_p and $\bar{\gamma}_q$ is average value of the SNRs γ_q. From (7), (9), and (10), the end-to-end SNR's PDF $f_\gamma(\gamma)$, is computed as (11).

$$f_\gamma(\gamma) = \frac{1}{8\pi\sigma_s^2\gamma}\int_0^\infty exp\left(-\frac{(ln(\frac{t}{\bar{\gamma}_p})+\sigma_s^2)^2}{8\sigma_s^2}\right) \times exp\left(-\frac{(ln(\frac{\gamma}{\bar{\gamma}_q t})+\sigma_s^2)^2}{8\sigma_s^2}\right)\frac{1}{t}dt \tag{11}$$

We solve the integral in (11) and obtain (12).

$$f_\gamma(\gamma) = \frac{ln(\gamma)}{8\pi\sigma_s^2\gamma} exp\left(-\frac{2\,ln(\frac{\gamma}{\bar{\gamma}})[1+\sigma_s^2]+2\sigma_s^4}{8\sigma_s^2}\right) \tag{12}$$

4. ASER ANALYSIS

We consider the ASER of FSO system that uses SC-QAM over atmospheric disorder. It is computed as (13) [17]:

$$\bar{P} = \int_0^{+\infty} P(\gamma) f_\gamma(\gamma) d\gamma \tag{13}$$

where $P(\gamma)$ is the conditional error probability (CEP). For using SC-QAM modulation, the CEP presented as (14):

$$P(\gamma) = 1 - [1 - 2q(M_I)Q(A_I)\sqrt{\gamma}]\left[1 - 2q(M_Q)Q(A_Q\sqrt{\gamma})\right] \tag{14}$$

where

$$A_I = \sqrt{6/\left[(M_I^2 - 1) + r^2(M_Q^2 - 1)\right]},$$

$$A_Q = \sqrt{6r^2/\left[(M_I^2 - 1) + r^2(M_Q^2 - 1)\right]},$$

$$q(x) = 1 - \frac{1}{x},$$

$Q(x) = \frac{1}{2} erfc(x/\sqrt{2})$ is Gaussian Q-function, $r = \frac{d_Q}{d_I}$ is quadrature to in-phase decision distance ratio, M_I is in-phase and quadrature signal amplitudes, respectively, M_Q is quadrature signal amplitudes. The (13) can be represented as (15):

$$\begin{aligned}\bar{P}(\gamma) &= \int_0^\infty 2q(M_I)Q(A_I\sqrt{\gamma})\frac{\ln(\gamma)}{8\pi\sigma_s^2\gamma}\exp\left(-\frac{2\ln(\frac{\gamma}{\bar{\gamma}})\left[1+\sigma_s^2\right]+2\sigma_s^4}{8\sigma_s^2}\right)d\gamma \\ &+ \int_0^\infty 2q(M_Q)Q(A_Q\sqrt{\gamma})\frac{\ln(\gamma)}{8\pi\sigma_s^2\gamma}\exp\left(-\frac{2\ln(\frac{\gamma}{\bar{\gamma}})\left[1+\sigma_s^2\right]+2\sigma_s^4}{8\sigma_s^2}\right)d\gamma \\ &- \int_0^\infty 4q(M_I)q(M_Q)Q(A_I\sqrt{\gamma})Q(A_Q\sqrt{\gamma})\frac{\ln(\gamma)}{8\pi\sigma_s^2\gamma}\exp\left(-\frac{2\ln(\frac{\gamma}{\bar{\gamma}})\left[1+\sigma_s^2\right]+2\sigma_s^4}{8\sigma_s^2}\right)d\gamma\end{aligned} \quad (15)$$

5. NUMERICAL RESULTS AND DISCUSSION

This section presents numerical results for RIS-assisted FSO systems' ASER analysis utilizing rectangular quadrature amplitude modulation and an avalanche over weak atmospheric turbulence channels modeled by a log-normal distribution. We use expressions that are derived in previous sections. ASER is computed as a transmitted optical power's function, P_t. This approach assures fair comparison. Many different operating conditions are investigated when the performance analysis: link distance, transmitted optical power, and rectangular quadrature amplitude modulation schemes. We can see the parameters of the analysis in Table 1.

Table 1. System parameters and constants

Parameters	Symbol	Value
Operational wavelength	λ	1550 nm
Index of refraction structure	C_n^2	$10^{-15}m^{-2/3}$
Link distance	L	1 ÷ 6 km
Aperture diameter	D	0.06 m

We analyze the average SNR versus ASER with different link distances, transmitted optical power, and QAM scheme. Figures 3 and 4 show the mathematical results of the scenarios. The causes can be explained: while the quadrature-to-in phase decision distance ratio decreases by increasing the modulation level. Therefore, the ASER of the FSO system will become worse. So, when using the high modulation level and still ensuring a low ASER, it must increase the transmitted optical power.

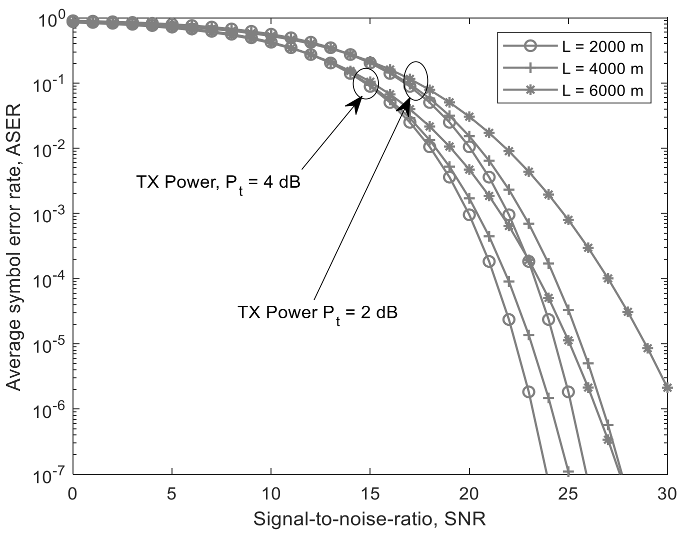

Figure 3. Average SNR versus ASER with different link distances and transmitted optical power

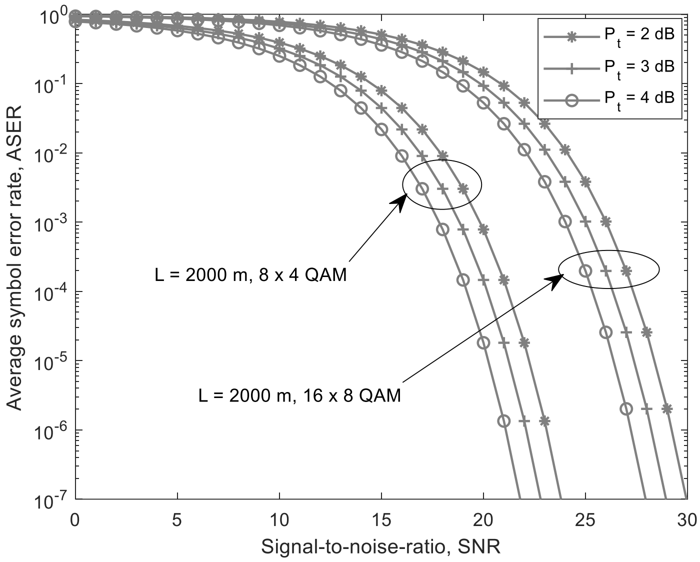

Figure 4. Average SNR versus ASER with different of transmitted optical power and QAM scheme

Figure 5 shows that ASER is an average electrical SNR function for different QAM schemes. We consider the case with RIS and without RIS. The ASER declines with the growth of the SNR, RIS-assisted, and reduces QAM schemes. The influence of the RIS-assisted on the system's performance is much more influential in high SNR regions than in low regions. Simulation results and analytical results are closed agreement.

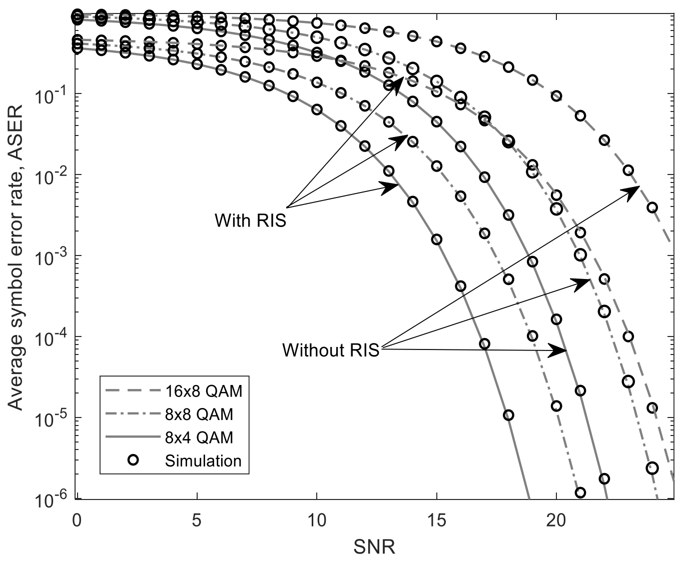

Figure 5. ASER performance compared with average SNR for values of QAM schemes

6. CONCLUSION

This study analyzes the ASER of RIS-assisted FSO system using the QAM modulation scheme over log-normal atmospheric turbulence channels. We propose theoretical expressions for RIS-assisted FSO systems considering different transmitted optical power, link distance, and QAM modulation scheme. It can see a significant improvement if deploying the RIS technique. That solves the LOS transmission problem. The numerical results pointed out that using RIS with transmitted optical power' proper selection improves the system significantly. In this study, the QAM schemes reach the best ASER of the system.

REFERENCES

[1] H. Kaushal and G. Kaddoum, "Optical communication in space: challenges and mitigation techniques," *IEEE Communications Surveys and Tutorials*, vol. 19, no. 1, pp. 57–96, 2017, doi: 10.1109/COMST.2016.2603518.

[2] A. K. Majumdar and J. C. Ricklin, *Free-space laser communications*. New York, NY: Springer New York, 2008.

[3] L. C. Andrews, R. L. Phillips, and C. Y. Young, *Laser beam scintillation with applications*. SPIE, 2001.

[4] A. García-Zambrana, C. Castillo-Vázquez, and B. Castillo-Vázquez, "Outage performance of MIMO FSO links over strong turbulence and misalignment fading channels," *Optics Express*, vol. 19, no. 14, Jul. 2011, doi: 10.1364/OE.19.013480.

[5] I. E. Lee, Z. Ghassemlooy, W. P. Ng, and M. Uysal, "Performance analysis of free space optical links over turbulence and misalignment induced fading channels," in *2012 8th International Symposium on Communication Systems, Networks and Digital Signal Processing (CSNDSP)*, Jul. 2012, pp. 1–6, doi: 10.1109/CSNDSP.2012.6292668.

[6] A. A. Farid and S. Hranilovic, "Outage capacity optimization for free-space optical links with pointing errors," *Journal of Lightwave Technology*, vol. 25, no. 7, pp. 1702–1710, Jul. 2007, doi: 10.1109/JLT.2007.899174.

[7] S. Arnon, "Effects of atmospheric turbulence and building sway on optical wireless-communication systems," *Optics Letters*, vol. 28, no. 2, Jan. 2003, doi: 10.1364/OL.28.000129.

[8] D. H. Ai and V. L. Nguyen, "BER analysis of amplify-and-forward relaying FSO systems using APD receiver over strong atmospheric turbulence channels," *International Journal of Electrical and Computer Engineering (IJECE)*, vol. 9, no. 5, pp. 3678–3686, Oct. 2019, doi: 10.11591/ijece.v9i5.pp3678-3686.

[9] C. K. Datsikas, K. P. Peppas, N. C. Sagias, and G. S. Tombras, "Serial free-space optical relaying communications over gamma-gamma atmospheric turbulence channels," *Journal of Optical Communications and Networking*, vol. 2, no. 8, Aug. 2010, doi: 10.1364/JOCN.2.000576.

[10] L. Kong, W. Xu, L. Hanzo, H. Zhang, and C. Zhao, "Performance of a free-space-optical relay-assisted hybrid RF/FSO system in generalized-distributed channels," *IEEE Photonics Journal*, vol. 7, no. 5, pp. 1–19, Oct. 2015, doi: 10.1109/JPHOT.2015.2470106.

[11] A. Basgumus, B. Hicdurmaz, H. Temurtas, M. Namdar, A. Altuncu, and G. Yilmaz, "Optimum transmission distance for relay-assisted free-space optical communication systems," *Optik*, vol. 127, no. 16, pp. 6490–6497, Aug. 2016, doi: 10.1016/j.ijleo.2016.04.070.

[12] K. O. Odeyemi and P. A. Owolawi, "On the performance of energy harvesting AF partial relay selection with TAS and outdated channel state information over identical channels," *International Journal of Electrical and Computer Engineering (IJECE)*, vol. 10, no. 5, pp. 5296–5305, Oct. 2020, doi: 10.11591/ijece.v10i5.pp5296-5305.

[13] K. P. Peppas, P. T. Mathiopoulos, and J. Yang, "On the effective capacity of amplify-and-forward multihop transmission over arbitrary and correlated fading channels," *IEEE Wireless Communications Letters*, vol. 5, no. 3, pp. 248–251, Jun. 2016, doi: 10.1109/LWC.2016.2530787.

[14] D. H. Ai, D. T. Quang, N. N. Nam, H. D. Trung, D. T. Tuan, and N. X. Dung, "Capacity analysis of amplify-and-forward free-space optical communication systems over atmospheric turbulence channels," in *2017 Seventh International Conference on Information Science and Technology (ICIST)*, Apr. 2017, pp. 103–108, doi: 10.1109/ICIST.2017.7926500.

[15] H. A. Duong, V. L. Nguyen, and K. T. Luong, "Misalignment fading effects on the ACC performance of relay-assisted MIMO/FSO systems over atmospheric turbulence channels," *International Journal of Electrical and Computer Engineering (IJECE)*, vol. 12, no. 1, pp. 966–973, Feb. 2022, doi: 10.11591/ijece.v12i1.pp966-973.

[16] D. H. Ai, "Average channel capacity of amplify-and-forward MIMO/FSO systems over atmospheric turbulence channels," *International Journal of Electrical and Computer Engineering (IJECE)*, vol. 8, no. 6, pp. 4334–4342, Dec. 2018, doi: 10.11591/ijece.v8i6.pp4334-4342.

[17] D. H. Ai, H. D. Trung, and D. T. Tuan, "On the ASER performance of amplify-and-forward relaying MIMO/FSO systems using SC-QAM signals over log-normal and gamma-gamma atmospheric turbulence channels and pointing error impairments," *Journal of Information and Telecommunication*, vol. 4, no. 3, pp. 267–281, Jul. 2020, doi: 10.1080/24751839.2020.1732734.

[18] M. Zeng, X. Li, G. Li, W. Hao, and O. A. Dobre, "Sum rate maximization for IRS-assisted uplink NOMA," *IEEE Communications Letters*, vol. 25, no. 1, pp. 234–238, Jan. 2021, doi: 10.1109/LCOMM.2020.3025978.

[19] M. A. ElMossallamy, H. Zhang, L. Song, K. G. Seddik, Z. Han, and G. Y. Li, "Reconfigurable intelligent surfaces for wireless communications: principles, challenges, and opportunities," *IEEE Transactions on Cognitive Communications and Networking*, vol. 6, no. 3, pp. 990–1002, Sep. 2020, doi: 10.1109/TCCN.2020.2992604.

[20] S. Atapattu, R. Fan, P. Dharmawansa, G. Wang, J. Evans, and T. A. Tsiftsis, "Reconfigurable intelligent surface assisted two-way communications: performance analysis and optimization," *IEEE Transactions on Communications*, vol. 68, no. 10, pp. 6552–6567, Oct. 2020, doi: 10.1109/TCOMM.2020.3008402.

[21] E. Basar, "Reconfigurable intelligent surface-based index modulation: a new beyond MIMO paradigm for 6G," *IEEE Transactions on Communications*, vol. 68, no. 5, pp. 3187–3196, May 2020, doi: 10.1109/TCOMM.2020.2971486.

[22] A. R. Ndjiongue, T. M. Ngatched, O. A. Dobre, and H. Haas, "Towards the use of re-configurable intelligent surfaces in VLC systems: Beam steering," *IEEE Wireless Communications*, vol. 28, no. 3, pp. 156–162, 2021.

[23] T. Ma, Y. Xiao, X. Lei, P. Yang, X. Lei, and O. A. Dobre, "Large intelligent surface assisted wireless communications with spatial modulation and antenna selection," *IEEE Journal on Selected Areas in Communications*, vol. 38, no. 11, pp. 2562–2574, Nov. 2020, doi: 10.1109/JSAC.2020.3007044.

[24] Z. Yigit, E. Basar, and I. Altunbas, "Low complexity adaptation for reconfigurable intelligent surface-based MIMO systems," *IEEE Communications Letters*, vol. 24, no. 12, pp. 2946–2950, Dec. 2020, doi: 10.1109/LCOMM.2020.3014820.

[25] C. U. Hail, A.-K. U. Michel, D. Poulikakos, and H. Eghlidi, "Optical Metasurfaces: evolving from passive to adaptive," *Advanced Optical Materials*, vol. 7, no. 14, Jul. 2019, doi: 10.1002/adom.201801786.

[26] L. Yang, F. Meng, J. Zhang, M. O. Hasna, and M. Di Renzo, "On the performance of RIS-assisted dual-hop UAV communication systems," *IEEE Transactions on Vehicular Technology*, vol. 69, no. 9, pp. 10385–10390, Sep. 2020, doi: 10.1109/TVT.2020.3004598.

[27] T. Ha Duyen and A. T. Pham, "Performance analysis of MIMO/FSO systems using SC-QAM signaling over atmospheric turbulence channels," *IEICE Transactions on Fundamentals of Electronics, Communications and Computer Sciences*, no. 1, pp. 49–56, 2014, doi: 10.1587/transfun.E97.A.49.

BIOGRAPHY OF AUTHORS

Duong Huu Ai he received the Master of Electronic Engineering from Danang University of Technology, Vietnam, in 2011, and the Ph.D. degree in Electronics and Telecommunications from Hanoi University of Technology, Vietnam, in 2018. Currently, he is a lecturer at Vietnam-the Korea University of Information and Communication Technology, The University of Danang, Vietnam. His research interests include optical wireless communications, optical and quantum electronics, 5G wireless communications and broadband networks, and IoT. He can be contacted at email: dhai@vku.udn.vn.

Cong Dat Vuong he received the Master of Telecommunication and Electronic from Sheffield Hallam University, Sheffield, U.K, in 2013. He got his Ph.D. degree from the school of Electronic Engineering, Soongsil University, South Korea, in 2018. His research interests include wireless communication, visible light communication, and antenna communication. He is currently a lecturer at Vietnam-the Korea University of Information and Communication Technology, The University of Danang, Vietnam. He can be contacted at email: vcdat@vku.udn.vn.

Dai Tho Dang he received the Master of Computer Sciences from the Nice Sophia Antipolis, France, in 2010, and the Ph.D. degree from Yeungnam University, Republic of Korea, in cooperation with the Wrocław University of Science and Technology, Poland, in 2020. Currently, he works as a lecturer at Vietnam-Korea University of Information and Communication Technology, The University of Danang, Vietnam. His research interests include statistical models, collective intelligence, and evolutionary computation. He can be contacted at email: ddtho@vku.udn.vn.